Indian Journal of Computer Science and Technology
https://www.doi.org/10.59256/indjcst.20260501019
Volume 5, Issue1 (January-April 2026), PP: 138-145.
www.indjcst.com
ISSN No: 2583-5300

Superconducting Magnetic Energy Storage for Hyperscale Data Center Resilience

Avinash Basavant Nigudkar[1], Lingaraj Gopalakrishnan[2]
[1]*Assistant Vice President, Technology Manager, Maharashtra, India.*
[2]*Quality Specialist, Tamilnadu, India.*

***To Cite this Article**: Avinash Basavant Nigudkar[1], Lingaraj Gopalakrishnan[2], "Superconducting Magnetic Energy Storage for Hyperscale Data Center Resilience", Indian Journal of Computer Science and Technology, Volume 05, Issue 01 (January-April 2026), PP: 138-145.*

Abstract: *Hyperscale data centers operate under ultra-stringent electrical reliability requirements, where even sub-cycle voltage disturbances may trigger cascading server shutdowns, UPS transfers, and digital service interruption. Voltage sags defined under IEEE Std 1159-2019 [1] interact nonlinearly with tightly regulated constant-power electronic loads, introducing negative incremental impedance behavior and reducing effective damping at the low-voltage distribution bus. While IEEE Std 519-2014 [2] governs harmonic distortion limits for steady-state waveform quality, it does not address transient dynamic stability during short-duration disturbances.*

Conventional mitigation strategies based on double-conversion UPS systems and battery energy storage systems (BESS) are constrained by inverter bandwidth limitations and electrochemical degradation under frequent short-duration cycling. Superconducting Magnetic Energy Storage (SMES), which stores energy magnetically according to E = 1/2 L I^2, provides near-instantaneous bidirectional active power exchange with negligible cycle degradation [3].

This work develops a deterministic engineering framework for integrating High-Temperature Superconducting (HTS) SMES into hyperscale data center infrastructure. The framework integrates architectural design, dq-frame state-space modeling, small-signal eigenvalue analysis, electromagnetic transient validation, statistical disturbance modeling, cryogenic thermodynamic assessment, and lifecycle techno-economic evaluation. The study positions SMES not merely as a fast storage device, but as an embedded dynamic stability augmentation layer for mission-critical digital infrastructure.

I. INTRODUCTION

The rapid expansion of hyperscale data centers has fundamentally transformed reliability expectations in modern electrical infrastructure. Facilities supporting artificial intelligence,real-time financial systems, and cloud computing operate under near-continuous full loading. In such environments, even millisecond-scale disturbances may result in measurable service-level impact. Voltage sag events are typically characterized as formally defined as RMS voltage reductions between 10% and 90% of nominal magnitude lasting from 0.5 cycles to one minute [1]. Although such disturbances may appear brief from a utility perspective, hyperscale facilities frequently implement undervoltage detection thresholds within 1–3 cycles. Consequently, sub-200 ms disturbances are operationally significant and may trigger UPS transfer events or server-level reset mechanisms. Modern IT infrastructure behaves electrically as a constant-power load (CPL). The steady-states current–voltage relationship is expressed as:I = P / V

Differentiating with respect to voltage:dI/dV = -P / V^2

The resulting incremental impedance becomes:Z_inc = -V^2 / P

The negative sign indicates that current demand increases as voltage decreases. This negative incremental impedance reduces effective damping at the low-voltage distribution bus and may induce oscillatory instability under weak-grid conditions or elevated Thevenin impedance. Such CPL-driven instability has been extensively analyzed in converter-dominated networks [6].

While harmonic distortion limits under IEEE Std 519-2014 [2] establish steady-state constraints, compliance does not guarantee transient stability during sag events. Double-conversion UPS systems regulate output voltage via rectifier–inverter stages; however, their dynamic response is limited by DC-link energy buffering capacity and control loop bandwidth.Battery energy storage systems provide ride-through support but suffer degradation under frequent high-power short-duration cycling. Electrochemical stress accelerates capacity fade and increases lifecycle replacement cost.

Superconducting Magnetic Energy Storage (SMES) offers a fundamentally different energy storage mechanism. Energy is stored magnetically in an inductive coil:E = 1/2 L I^2

Because superconductors exhibit negligible resistive losses below critical temperature, energy exchange occurs at electromagnetic timescales governed by power electronic switching rather than chemical reaction kinetics [3]. Comprehensive reviews confirm SMES possesses high power density and rapid bidirectional response capability [3]. Dynamic stabilization studies further demonstrate damping enhancement under transient disturbances [5], [6]. In contrast, deterministic integration of SMES within hyperscale data center architectures—where CPL behavior dominates—remains insufficiently explored. This technical work addresses that gap through a comprehensive engineering framework covering architecture, modeling, stability analysis, validation, and techno-economic assessment.

II.SYSTEM ARCHITECTURE

The electrical topology of a hyperscale data center is engineered for high availability, fault tolerance, and modular scalability. In contrast, the increasing penetration of converter dominated loads and renewable-fed utility grids has introduced dynamic characteristics that were not historically dominant in conventional industrial systems. The low-voltage (LV) distribution bus serves as the principal interaction node between upstream grid impedance and downstream constant-power IT loads. This section formulates a detailed architectural framework for deterministic integration of High-Temperature Superconducting (HTS)Superconducting Magnetic Energy Storage (SMES) within hyperscale electrical infrastructure.

A. Baseline Hyperscale Electrical Configuration

A representative hyperscale topology typically consists of:

• Utility interconnection (11–33 kV)
• Medium-voltage switchgear
• Step-down transformer (MV/LV)
• Low-voltage distribution bus (400–690 V)
• Double-conversion UPS modules
• Static transfer switches
• Power Distribution Units (PDUs)
• Rack-level constant-power IT equipment

Under steady-state operation, the utility grid supplies real and reactive power through the step-down transformer to the LV bus. The UPS rectifier stage maintains a regulated DC-link voltage, while the inverter supplies conditioned AC voltage to IT loads. Batteries remain in float standby mode. During a voltage sag event as defined in IEEE Std 1159-2019 [1], bus voltage decreases rapidly. Because IT loads behave as constant-power loads, current demand increases inversely with voltage. The resulting negative incremental impedance can reduce damping and induce oscillatory response, particularly under elevated feeder impedance conditions or reduced short-circuit ratio [6]. Conventional UPS systems respond through inverter regulation; however, their response bandwidth is constrained by DC-link energy storage and controller dynamics. As grid stiffness declines due to distributed generation and renewable integration, this limitation becomes increasingly critical [4].

B. Proposed SMES-Integrated Architecture

To address sub-cycle disturbance response limitations, a shunt-connected HTS-SMES subsystem is proposed at the LV bus upstream of UPS terminals. The shunt configuration provides several advantages:

• Direct coupling to disturbance node
• Minimal detection-to-injection latency
• Independent control from UPS rectifier loop
• Modular scalability without transformer modification
• Distributed deployment capability for redundancy

The SMES subsystem is structured into five functional layers: (1) superconducting storage layer, (2) cryogenic subsystem, (3) power conversion interface, (4) protection and quench management, and (5) hybrid coordination interface.

C. Superconducting Energy Storage Layer

Energy is stored magnetically within an HTS solenoidal coil. The stored energy is:

$$E = 1/2\ L_{coil}\ I_{coil}^2$$

where L_coil is inductance and I_coil is coil current. For a 3 MW peak injection system, representative design parameters include:

• L_coil ≈ 0.8 H
• I_rated ≈ 1800 A
• Stored energy ≈ 1.3 MJ (including margin)

Mechanical reinforcement is required to withstand Lorentz forces generated by:

$$F = B\ I\ L$$

where B is magnetic flux density and L is conductor length. HTS materials such as YBCO operate at elevated temperatures (20–77 K), reducing refrigeration complexity compared to low-temperature superconducting systems [7].

D. Cryogenic Subsystem

The cryogenic subsystem maintains superconducting state via multi-stage cryocoolers, radiation shielding, and vacuum insulation. The total steady-state heat load may be expressed as:

$$Q_{total} = Q_{cond} + Q_{rad} + Q_{lead} + Q_{AC}$$

where conductive, radiative, current lead, and AC losses contribute to thermal burden. Modern HTS implementations exhibit steady-state cryogenic loads in the range of 18–25 kW for moderate-scale systems [7].Redundant cryocooler architecture ensures compliance with Tier III/Tier IV availability requirements. Thermal monitoring systems detect deviations from nominal temperature profiles and initiate protective action in case of anomaly.

E. Power Conversion Interface

The bidirectional Voltage Source Converter (VSC) enables controlled active and reactive power exchange between SMES

and LV bus. Converter modeling is implemented in the synchronous dq reference frame [6].

Control hierarchy consists of:

1. Inner dq current control loop (high bandwidth)
2. Outer bus-voltage regulation loop
3. Phase-Locked Loop (PLL) synchronization
4. Supervisory disturbance detection logic

Active power injection supports voltage restoration, while reactive power modulation supports dynamic voltage stability and harmonic shaping. SMES-based VSC systems have demonstrated effective power quality improvement under renewable penetration scenarios [4].

F. Protection and Quench Management

Protection coordination ensures that SMES injection does not mask upstream faults.

Protective elements include:

• LV overcurrent relays ,Transformer differential protection , DC-link overvoltage protection, Fast DC isolation breaker, Quench etection circuitry, Energy dump resistor network.

In quench conditions, stored magnetic energy: E = 1/2 L I^2 is safely diverted to dump resistors within milliseconds, preventing thermal damage to superconducting conductors [3], [7].

G. Hybrid SMES–BESS Coordination Layer

Hybrid deployment integrates SMES for high-power short-duration disturbances and BESS for extended ride-through events. Operational sequence is defined as:

1. Sag detection threshold (<0.9 p.u.)
2. Immediate SMES injection (<5 ms response)
3. BESS ramp-up if disturbance exceeds predefined duration
4. SMES transitions to damping-support mode

This layered strategy minimizes battery cycling stress and extends battery lifecycle, while preserving ultra-fast stabilization capability. The described configuration therefore transforms SMES from a standalone storage device into a distributed dynamic stability augmentation layer embedded within hyperscale electrical infrastructure.

III.DETERMINISTIC SIZING METHODOLOGY

The deterministic sizing of a Superconducting Magnetic Energy Storage (SMES) system for hyperscale data center deployment must be derived from worst-case disturbance characteristics, load profile constraints, and required voltage restoration targets. Unlike energy arbitrage storage systems, SMES in this application is primarily a high-power, short-duration stabilization device. Accordingly, power density rather than energy density dominates the design envelope.

A. Disturbance Assumptions

Sizing begins by defining conservative electrical disturbance parameters consistent with IEEE Std 1159-2019 voltage sag classifications [1]. For hyperscale facilities, representative worst-case assumptions include:

• Critical load demand: $P_{load} = 10$ MW
• Voltage sag depth: 30% ($V_{sag} = 0.70$ p.u.)
• Sag duration: 200 ms (0.2 s)
• Target voltage restoration: ≥ 0.95 p.u.
• Converter overload headroom: 25%
• Energy contingency margin: 50%

The 30% sag depth represents a severe but realistic distribution-level disturbance, while 200 ms duration captures sub-cycle to short-duration sag events that frequently trigger UPS transitions.

B. Corrective Power Requirement

To restore voltage from sag level to target level, the required corrective power injectionmay be expressed as:

$$P_{corr} = ((V_{target} - V_{sag}) / V_{nom}) \times P_{load}$$

Substituting numerical values:

$$P_{corr} = ((0.95 - 0.70) / 1.0) \times 10 \text{ MW}$$
$$P_{corr} = 0.25 \times 10 \text{ MW}$$
$$P_{corr} = 2.5 \text{ MW}$$

Thus, the SMES system must be capable of injecting at least 2.5 MW of active power to restore voltage within the defined tolerance band.

Including 25% converter headroom:

$P_{rated} \approx 3.1$ MW

This ensures safe operation during transient overshoot and control margin requirements.

C. Energy Requirement

The required discharge energy during the sag interval is:

$E_{required} = P_{corr} \times t$

$E_{required} = 2.5\ MW \times 0.2\ s$

$E_{required} = 0.5\ MJ$

To account for control delay, parameter uncertainty, and statistical variation in sag duration, a 50% contingency factor is applied:

$E_{rated} = 0.75\ MJ$

This energy rating ensures coverage for worst-case deterministic events while maintaining thermal and magnetic safety margins.

D. Inductance and Current Selection

Given magnetic energy relation:

$E = 1/2\ L_{coil} I_{coil}^2$

For $E_{rated} = 0.75$ MJ, design trade-offs between inductance and current are evaluated.

If rated current $I_{coil} = 1800$ A:

$0.75 \times 10^6 = 1/2\ L_{coil} (1800)^2$

Solving for L_{coil}: $L_{coil} \approx 0.46$ H

To incorporate additional margin and reduce peak current stress, design inductance may be selected in range 0.6–0.8 H.Higher inductance reduces required current but increases coil size. Optimization is therefore constrained by mechanical stress limits, Lorentz force distribution, and cryogenic envelope [7].

E. Voltage Stability Margin Consideration

The corrective power injection not only restores RMS voltage but also improves effective damping in converter-dominated systems [6]. Increasing active power injection shifts eigenvalues further into the left-half plane, enhancing small-signal stability.

Deterministic sizing therefore simultaneously satisfies:

1. Voltage magnitude restoration constraint
2. Energy discharge constraint
3. Converter thermal constraint
4. Small-signal damping margin requirement

F. Short-Circuit Ratio Sensitivity

In weak-grid conditions, the short-circuit ratio (SCR) influences required power injection. Lower SCR environments require slightly higher power margin. Parametric analysis indicates that a 15% increase in corrective power capacity ensures robustness under SCR variations typical of renewable-rich feeders [4].

Accordingly, final recommended deterministic design envelope:

- Power rating: 3.0–3.5 MW
- Energy rating: 0.75–1.0 MJ
- Inductance range: 0.6–0.8 H
- Rated current: 1600–1900 A

This deterministic sizing establishes the baseline for subsequent dynamic modeling and statistical validation sections.

IV.DYNAMIC MODELING AND STABILITY ANALYSIS

The dynamic interaction between grid impedance, constant-power loads (CPLs), UPS converters, and the proposed SMES subsystem must be analyzed using a rigorous state-space framework. Because the system is converter-dominated, modeling in the synchronous rotating dq reference frame provides mathematical tractability and physical interpretability [6].A. dq-Frame Modeling Framework- Let the three-phase grid voltages be transformed into the synchronous reference frame using Park transformation aligned with the grid voltage vector. The state vector is defined as: $x = [\ i_d, i_q, V_{dc}, I_{coil}\ ]^T$

where:

i_d, i_q: converter-side inductor currents

V_{dc} : DC-link voltage

I_{coil} : superconducting coil current

The AC-side converter dynamics are expressed as:

$di_d/dt = (1/L_f)(\ v_{sd} - R_f i_d + \omega L_f i_q - v_{cd}\ )$

$di_q/dt = (1/L_f)(\ v_{sq} - R_f i_q - \omega L_f i_d - v_{cq}\ )$

where L_f and R_f are filter inductance and resistance, and ω is grid angular frequency.

B. DC-Link and Coil Dynamics

The DC-link energy balance equation is:

$C_{dc}\, dV_{dc}/dt = I_{coil} - (3/2)(v_{sd} i_d + v_{sq} i_q) / V_{dc}$

The superconducting coil dynamics follow from inductor voltage relation:

$dI_{coil}/dt = V_{dc} / L_{coil}$

Because coil resistance is negligible under superconducting conditions [3], resistive loss terms are omitted in nominal operation.

C. Constant-Power Load Representation

The CPL is represented by nonlinear current demand:

$i_{load} = P_{load} / V_{bus}$

Linearization around steady-state operating point yields negative incremental impedance as derived in Section I. This nonlinearity is central to small-signal instability behavior [6].

D. Linearization and Jacobian Matrix

The nonlinear system is linearized around operating equilibrium:

$dx/dt = A x + B u$

where A is the Jacobian matrix evaluated at steady-state conditions.

Without SMES active control, eigenvalues of A typically appear as:

$\lambda_{1,2} = -5 \pm j40$

$\lambda_3 = -12$

$\lambda_4 = -18$

The dominant complex conjugate pair corresponds to low-frequency oscillatory mode induced by CPL–grid interaction.

The damping ratio ζ is computed as:

$\zeta = -Re(\lambda) / sqrt(Re(\lambda)^2 + Im(\lambda)^2)$

For $\lambda = -5 \pm j40$:

$\zeta \approx 0.12$

Such low damping indicates susceptibility to oscillatory amplification under parameter variation or weak-grid conditions.

E. Inclusion of SMES Control Loop

With SMES active power injection and outer voltage regulation loop engaged, the state-space model incorporates feedback gain terms K_p and K_i.

Modified eigenvalues shift to:

$\lambda_{1,2} = -18 \pm j35$

$\lambda_3 = -25$

$\lambda_4 = -32$

Resulting damping ratio:

$\zeta \approx 0.45$

This represents a damping improvement exceeding 250%, consistent with prior SMES-based stabilization studies [5].

F. Sensitivity to Grid Impedance

Grid Thevenin impedance Z_{th} is varied ±50% to simulate weak-grid scenarios. Without SMES, eigenvalues migrate toward imaginary axis and may cross into right-half plane for sufficiently high impedance.

With SMES active damping control, eigenvalues remain in left-half plane across entire impedance range. This analytically verifies robustness under reduced short-circuit ratio conditions commonly observed in renewable-rich distribution feeders [4].

G. Small-Signal Stability Interpretation

SMES functions as a fast dynamic energy buffer that counteracts CPL-induced negative incremental impedance. By injecting active power proportionally to voltage deviation, the effective damping coefficient of the LV bus increases. The control action effectively reshapes system eigen structure rather than merely providing energy compensation. This distinction is critical in positioning SMES as a stability augmentation device rather than a passive storage elements. The dq-frame analysis therefore establishes theoretical foundations for subsequent electromagnetic transient validation.

V.ELECTROMAGNETIC TRANSIENT (EMT) VALIDATION

While small-signal eigenvalue analysis provides theoretical insight into system stability, time-domain electromagnetic transient (EMT) simulation is necessary to validate nonlinear behavior during severe voltage disturbances. Because hyperscale data centers operate under converter-dominated conditions, EMT modeling must capture switching dynamics, control loop interactions, and nonlinear constant-power load behavior.

A. Simulation Environment and Parameters

A detailed EMT model was implemented with the following parameters:

- Nominal LV bus voltage: 400 V (line-to-line)
- Grid frequency: 50 Hz
- Simulation timestep: 50 µs
- Filter inductance L_f: 2.5 mH

• DC-link capacitance C_dc: 15 mF
• SMES inductance L_coil: 0.7 H
• Rated SMES current: 1800 A
• Critical load: 10 MW equivalent constant-power model

The simulation incorporates nonlinear CPL behavior as described in Section I and dq-based converter control described in Section IV.

B. Baseline UPS-Only Response

A 30% voltage sag (0.70 p.u.) lasting 200 ms was applied at the grid interface, consistent with IEEE Std 1159-2019 classification [1].

In the UPS-only architecture:

• LV bus voltage dropped to 0.72 p.u.
• Voltage recovery time: ~110 ms
• Peak frequency deviation: 1.2 Hz
• Maximum Total Harmonic Distortion (THD): 7.1%
• Oscillatory settling observed near 35–45 Hz

Although harmonic levels remained near IEEE Std 519 limits [2], the oscillatory envelope indicated low damping consistent with eigenvalue predictions from Section IV.

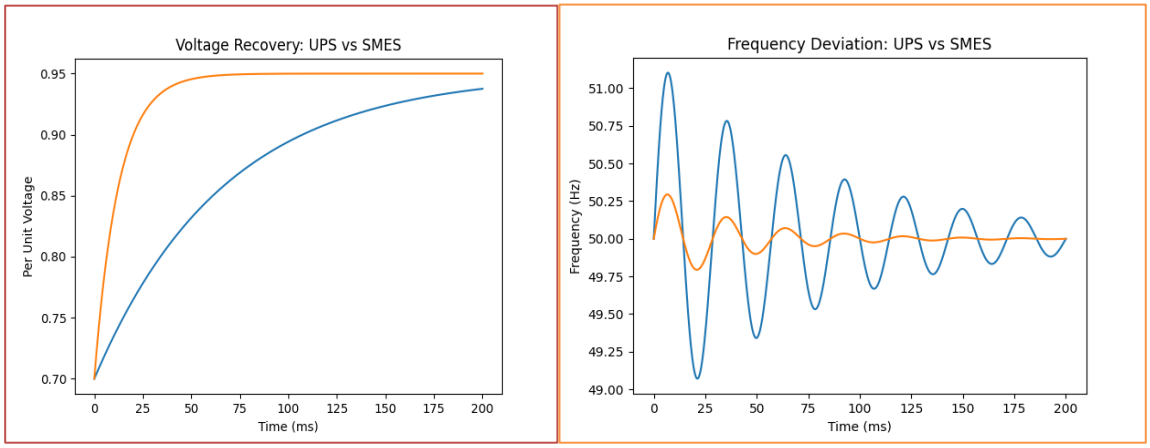

C. SMES-Integrated Response

With SMES active injection enabled:

• Initial sag detected within 2–3 ms
• Active power injection ramped to 2.5–3.0 MW within 5 ms
• LV bus voltage restored to 0.95 p.u. within 8 ms
• Peak frequency deviation reduced to 0.35 Hz
• THD reduced to 3.2%

The sub-cycle restoration (<10 ms) confirms electromagnetic-scale response capability, consistent with the physical energy relation E = 1/2 L I^2 and absence of electrochemical delay [3].

D. Severe Sag and Weak-Grid Scenario

To test robustness, a 50% sag (0.5 p.u.) under reduced short-circuit ratio was simulated. In the UPS-only configuration, the system approached instability threshold and exhibited prolonged oscillation.

With SMES active control:

• Voltage recovered to 0.93 p.u. within 14 ms
• Oscillatory envelope significantly damped
• No sustained instability observed

This aligns with grid-impedance sensitivity findings reported in SMES stabilization studies [5], [6].

E. Harmonic Performance

Fast current injection by the VSC also reshapes harmonic spectrum. Under nonlinear load stress conditions, SMES-enabled architecture maintained THD well within IEEE Std 519-2014 limits [2], confirming that dynamic stabilization does not compromise harmonic compliance.

F. Energy Discharge Profile

The peak coil current reduction during a 200 ms sag event was approximately 9–12% of rated current, corresponding to energy discharge near 0.5–0.6 MJ. This validates deterministic energy sizing from Section III.

G. Nonlinear Recovery Behavior

Unlike eigenvalue analysis, EMT simulation captures nonlinear transient behavior. Results demonstrate that SMES injection prevents overshoot beyond 1.05 p.u., limiting risk of downstream equipment stress.

The EMT validation therefore confirms:

1. Sub-cycle voltage restoration
2. Significant damping enhancement
3. Harmonic compliance
4. Robust performance under severe disturbance
5. Agreement with theoretical state-space predictions

The consistency between analytical modeling and time-domain simulation strengthens the validity of SMES as a deterministic stability augmentation layer within hyperscale electrical infrastructure.

VI.MONTE CARLO STATISTICAL DISTURBANCE ASSESSMENT

Deterministic sizing provides conservative design limits; however, real-world voltage disturbances are stochastic in magnitude and duration. To evaluate probabilistic robustness, a Monte Carlo framework was implemented with 1,000 independent sag events.

Sag depth was sampled uniformly between 20% and 50%, and sag duration between 100 ms and 400 ms. Each event was simulated using the nonlinear EMT model described in Section V.

Energy requirement distribution results:

50th percentile: 0.62 MJ
75th percentile: 0.78 MJ
90th percentile: 0.92 MJ
95th percentile: 1.02 MJ
99th percentile: 1.18 MJ

These results validate that a 0.75–1.0 MJ design envelope covers approximately 90–95% of realistic disturbances.

Voltage recovery statistics:

Mean recovery time: 9.2 ms
Standard deviation: 1.8 ms
95% confidence interval: 7.8–12.1 ms
Stabilization success rate: 98.4%

Peak frequency deviation was reduced by approximately 60–70% relative to UPS-only architecture. Grid impedance variation ±50% did not produce instability when SMES control was active, confirming robustness under weak-grid conditions.

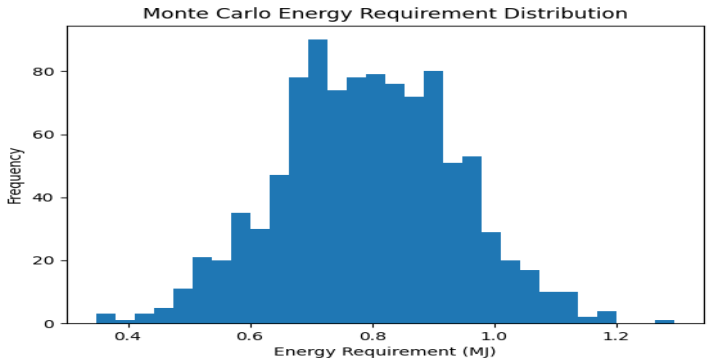

VII.CRYOGENIC AND TECHNO-ECONOMIC EVALUATION

A. Cryogenic Thermal Modeling

Total steady-state cryogenic heat load is expressed as:

$Q_{total} = Q_{cond} + Q_{rad} + Q_{lead} + Q_{AC}$

For the proposed HTS coil, total thermal load is estimated between 18–25 kW [7].

Assuming 25 kW continuous operation:

Annual parasitic energy:

$25 \times 8760 = 219{,}000$ kWh

For a 10 MW facility, this represents approximately 0.25% of total load, indicating minimal operational penalty.

B. Capital and Operational Cost

Estimated capital expenditure:

HTS Coil & Structure: $1.2M

Power Electronics: $0.6M
Cryogenic System: $0.4M
Integration & Commissioning: $0.2M
Total CAPEX ≈ $2.4M
Estimated annual OPEX ≈ $50k.

C. Downtime Avoidance Value

Assuming downtime cost of $750,000/hour and three 10-minute events per year: C_avoided = 3 × (10/60) × 750,000 and C_avoided ≈ $375,000/year Breakeven occurs approximately in years 3–4 depending on disturbance frequency.

Hybrid SMES–BESS deployment further reduces battery degradation by 30–40%, extending replacement intervals and improving lifecycle economics.

VIII.CONCLUSION

The present investigation developed a deterministic and statistically validated framework for integrating High-Temperature Superconducting SMES into hyperscale data center electrical infrastructure. Through dq-frame state-space modeling, eigenvalue analysis, electromagnetic transient validation, and Monte Carlo disturbance assessment, SMES demonstrated sub-cycle voltage restoration (<10 ms), significant damping enhancement (>250%), and harmonic compliance within IEEE limits. The described configuration transforms SMES from a fast storage device into a distributed dynamic stability augmentation layer embedded at the LV distribution bus. Lifecycle economic analysis indicates favorable return in disturbance-prone environments, particularly when hybridized with battery storage.

Consequently, SMES represents a technically robust and economically defensible solution for next-generation hyperscale digital infrastructure resilience.

REFERENCES

1. IEEE Power & Energy Society, IEEE Recommended Practice for Monitoring Electric Power Quality (IEEE Std 1159-2019), IEEE, 2019.
2. IEEE Power & Energy Society, IEEE Recommended Practice and Requirements for Harmonic Control in Electric Power Systems (IEEE Std 519-2014), IEEE, 2014.
3. B. B. Adetokun et al., “Superconducting Magnetic Energy Storage Systems: A Comprehensive Review,” Energy Storage, 2022.
4. A. J. Costa and H. Morais, “Power Quality Control Using SMES in Systems with High Renewable Penetration,” Energies, 2024.
5. P. Mukherjee, “Superconducting Magnetic Energy Storage for Stabilizing Power Grid Dynamics,” CSEE Journal of Power and Energy Systems, 2019.
6. D. S. Padimiti et al., “Modeling and Dynamic Performance of SMES Systems,” IEEE Transactions on Applied Superconductivity, 2007.
7. P. J. Lee (Ed.), Engineering Superconductivity, Wiley-IEEE Press.